

A Force Controlled Under Actuated Robotic Hand with Mechanical Intelligence and Proprioceptive Compliant Actuation

Xiaoguang Zhang, Taoyuanmin Zhu, Itsui Yamayoshi and Dennis Hong¹

Abstract—A three-finger under actuated robotic hand with dexterous force control and inherent compliance is developed and tested. A simplified biomimetic finger design is generated and applied, with mechanical intelligence principles carefully designed and embedded such that optimal trajectories for grabbing are naturally followed and the fingers can automatically conform to the goal object. A generalizable potential energy flow theory is then proposed to explain the mechanism behind the mechanical intelligence. The theory is also supported by experimental results. Quasi-direct drive actuators were developed to actuate the robotic hand with proprioceptive force sensing and inherent compliance. The hand performs delicate force controlled manipulation with a simple compliance controller implemented.

I. INTRODUCTION

Manipulators are an essential aspect of a robot's ability to interface with their working environments in order to finish their tasks. Often times these working environments are designed for human beings. Thus, for robots to finish the tasks they are designed for, robotic hands with biomimetic fingers are almost always the preferred design, such as the The DLR robotic hand [1] and the the ADROIT robotic hand [2]. These designs attempt to mimic human fingers using full actuation, where each joint is independently actuated and controlled, resulting in redundant actuation and very complicated, heavy, and bulky systems. However, many simple grasping and manipulation tasks don't require full actuation, meaning these complex hands are unnecessarily increasing the payload of the arm. As such, fully actuated robotic hands are conventionally not preferred, and robotic hands such as the tendon driven SDM hand by Dollar [3] and the four-bar linkage driven robotic grasping hand by Gosselin [4] which feature fewer fingers and under actuated finger designs have been developed.

These under actuated systems significantly reduced the size, weight and complexity of robotic manipulators while still retaining their utility. However, a drawback of under actuation is that there is some uncertainty in the trajectory of the fingers. This problem can be solved by embedding mechanical intelligence, which reduces the difficulties of finger control while also improving the quality of the manipulation. Mechanical intelligence in under actuated system was first introduced about 30 years ago [5], but still has a relatively blurred definition.

*This work was partially supported by the ONR through grant N00014-15-1-2064.

¹All authors are with the Robotics and Mechanisms Laboratory (RoMeLa) at the University of California, Los Angeles (UCLA), Los Angeles, CA 90095, USA. The corresponding author can be reached at hawkblizzard@g.ucla.edu.

Previous researchers have tried to explain the mechanism of mechanical intelligence by embedding it in their specific systems via kinematics and force equations [5] or screw theory [6], but the results are usually limited to their own setups and are generally not scalable or applicable in other under actuated mechanical systems.

Further, implementing force control on robotic hands to perform dexterous grasping and manipulation has also been a difficult problem, especially for fragile objects. Many research groups have done remarkable research on force controlled manipulators by applying tactile sensors [7], artificial skin [8] or force/torque (FT) sensors on finger [9] or wrist [10] joints. However, even though these methods performed admirably for the tasks they were designed for, the sensor systems used were always difficult to fabricate or expensive, and required large computational resources to support a high control frequency that was essential for the success of these types of robotic hand systems. On top of that, these systems usually performed poorly when dealing with external impulses or when approaching a goal object at high speeds, since either the system itself or the goal object would likely be damaged.

In this paper, we introduce a new force controlled under actuated robotic hand with mechanical intelligence and proprioceptive compliant actuation called DAnTE (Dynamic Anthropomorphic Tactile End-effector). This robotic hand system has fingers with simplified biomimetic design which take the advantages of the human finger tendon drive system while still being under actuated to reduce hardware and software complexities. The finger systems on DAnTE possess carefully designed mechanical intelligence such that the partition of the fingers trajectory from the under actuated DoF is controlled by the mechanical intelligence. We also provided a potential energy flow point of view to explain the mechanism behind the mechanical intelligence, which we think has the potential to be scaled or applied on other types of mechanical systems with under actuated DoF.

A quasi-direct drive [11] actuation system developed recently in our lab is adapted into DAnTE to provide inherent compliance and proprioceptive force sensing. By taking advantage of the high resolution current sensing and responsive control on the quasi-direct drive actuation system, we are able to achieve fast and dexterous force controlled grasping and manipulation without using any FT sensor. This actuation system also provides intrinsic compliance in the finger joints, providing the robotic hand system with excellent performance when it comes to fragile objects or impulses.

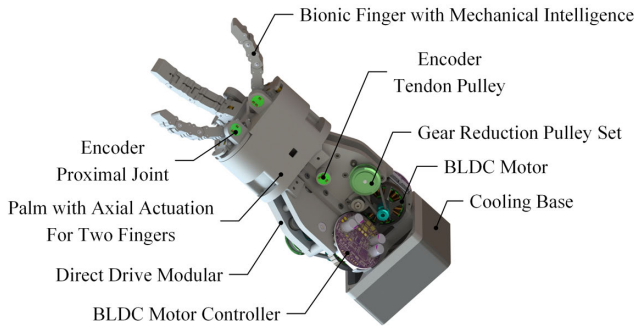


Fig. 1: Structure of the end-effector system. The system contains a hand assembly and an actuation assembly. Details of the two assemblies are shown above.

II. MECHANICAL DESIGN

DAnTE contains a hand assembly and an actuation assembly. The hand assembly is composed by a palm assembly and three fingers, while the actuation assembly is simply composed by three identical actuation assemblies, with each finger on the hand independently driven by an actuator. Fig.1 is an overview of the system, and the mechanical design is described in detail in the following sections.

The overall system specifications of DAnTE is as shown in table.I Note that the maximum fingertip force is limited to 30N because this prototype is FDM 3D printed with ABS, and a force exceeding this maximum will damage the internal tendon structure.

TABLE I: Specifications of DAnTE robotic hand platform.

Parameters	Value
Weight	1.5 kg
Overall Length w/o Finger	26 cm
Finger Length	90 mm
Object Diameter	0-120 mm
Max. Fingertip Force	30 N
Min. Retraction Time	300 ms

A. Palm

There are three fingers mounted axisymmetrically on the palm, with two of them able to rotate along their own central axis so that different relative positions of the three fingers can be achieved. These two fingers are coupled by gears and are driven by a single servo so that they always mirror each other. The palm also acts as the housing for a servo and the corresponding powertrain for finger orientation actuation. The finger orientation actuation powertrain is as shown in Fig.2. Both actuated fingers have a 90 degree range of motion along their own central axis, forming all grasping gestures as shown in Fig.3.

B. Simplified Biomimetic Finger

To better illustrate the design of the biomimetic finger, it's necessary to briefly review the functional anatomy of the extensor and flexor mechanism of human finger. As



Fig. 2: Finger axial rotation powertrain contained in the palm.

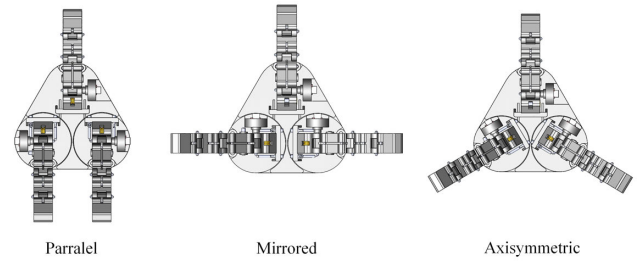


Fig. 3: The three basic gestures DAnTE can form for grasping tasks. The gestures are formed by changing the angular position of the two actuated fingers. The parallel configuration is preferred for prismatic objects while the asymmetric (tripod) gesture is often used for circular objects. The mirrored gesture is good for pinching operations.

shown in Fig.4 [12], tendon movements marked by the black arrows (such as retraction of EDC & EIP tendon) cause the finger extension, while tendon movements marked by the red arrows (such as retraction of the FDS tendon) cause finger flexion. The retraction of FDP tendon causes the distal and middle phalanges to bend, the retraction of FDS tendon causes the middle phalanx to bend, and the flexion of the proximal phalanx is done by the retraction of the extensor hood.

Clearly, a human finger is a complex fully actuated mechanism, and implementing a robotic hand with the same finger design may not be the best approach as it would require numerous actuators, a complicated tendon system, and a complex controller. The resulting platform would likely be cumbersome and lack robustness. Instead, we would like to adopt a simplified version of a human finger for our robotic hand.

The objective of DAnTE is to mainly do gripping and some simple manipulation, thus high agility on the fingers which would require the finger to be fully actuated is not necessary. There are three rotational DoF in a human finger, respectively on the DIP, PIP and MCP joint. Due to the coupling between the FDP tendon and the middle phalanx, in most cases, the distal and middle phalanges move correspondingly in free-load motions. In fact, in most grasping motions except fingertip grasping, corresponded bending on

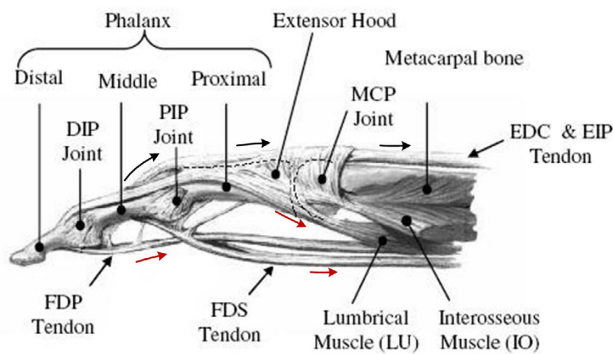
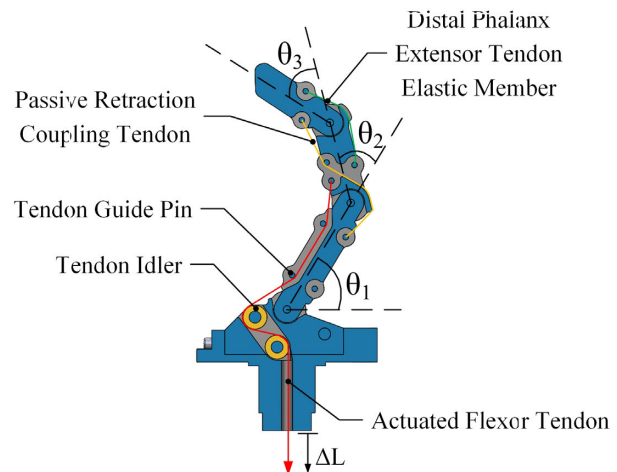


Fig. 4: Human finger tendon system mechanical structure. tendon movements marked by the black arrows cause the finger extension, while tendon movements marked by the red arrows cause finger flexion.

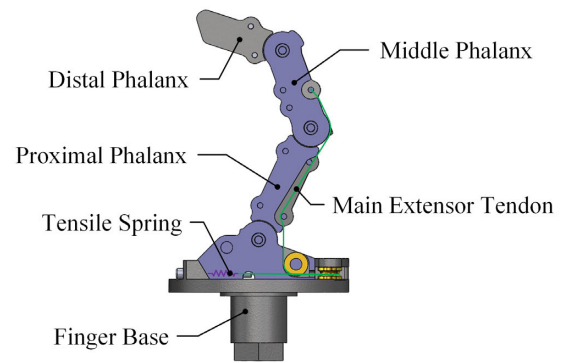
these two phalanxes is preferred for better grasping. Thus, we can simplify the coupling between the FDP tendon and the middle phalanx with a passive reaction coupling tendon, as the yellow tendon shown in Fig.5a. With this coupling tendon, the distal phalanx always bends together with the middle phalanx. The remaining two DoF are actuated by one actuated flexor tendon attached to the middle phalanx, as the red tendon shown in Fig.5a. The tendon goes under two tendon guide pins that are fixed on the proximal phalanx. The actuated flexor tendon drives both the middle phalanx and the proximal phalanx by directly pulling the middle phalanx and using the normal force on the tendon guide pins to drive the proximal phalanx. Since the main tasks of this grasper are about grasping and manipulation, it is not necessary for the extension motions of the fingers to be actuated, thus elastic members are used as extensor tendons. The extensor tendons are arranged to oppose the flexor tendons, with an elastic extensor tendon linking the distal and middle phalanx over the DIP joint to counteract the distal phalanx bending relative to the middle phalanx, keeping the passive reaction coupling tendon in tension. The other extensor tendon is the main extensor tendon, and is a rigid string attached to the back of the middle phalanx, going under a guide pin on the back of the proximal phalanx. It is then pulled by a tensile spring, as the red tendon shown in Fig.5b. The main extensor tendon recovers the middle and proximal phalanx from bending, keeping the actuated flexor tendon in tension.

C. Actuation Assembly

As mentioned before, the actuation assembly contains three direct drive actuation modules, with each of them driving one finger. The concept of our direct drive actuation module is to combine a brushless torque motor with very low gear reduction ratio. Fig.6 shows the main components in the actuator subassembly with all the structural parts and bearings hidden. T-Motor Antigravity 4004 brushless DC motors are employed, driving a two-step speed reduction transmission composed of two sets of timing pulleys, providing a total reduction ratio of 8.6:1. Each timing belt is



(a) Flexor



(b) Extensor

Fig. 5: Tendon system in the under actuated finger design. Figure(a) shows the mechanism of the flexor tendons (in red), while figure(b) shows the mechanism of the extensor tendons (in green).

associated with an adjustable tensioner. A tendon pulley is attached at the end of the powertrain to drive the tendon, and a 12-bit absolute encoder is also attached to the shaft of this tendon pulley so that the length of pulled part on the tendon can be precisely acquired. The BLDC motor is controlled by a motor controller developed and fabricated in house.

III. EMBEDDED MECHANICAL INTELLIGENCE

The principle of Mechanical intelligence is adopted in this under actuated finger design for automatic object conforming and optimal trajectory following. We would like to illustrate the mechanical intelligence respectively in both the flexor and extensor aspect.

Even though the finger is under actuated, the two DoF on the finger are constrained and coupled with each other by the actuated flexor tendon. Fig.7a shows a scenario in which the length of the tendon is fixed, and the fingers posture can only be along a certain trajectory depending on the loading

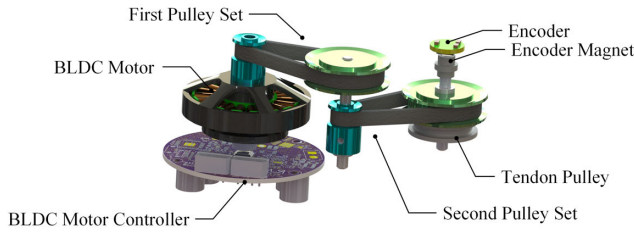
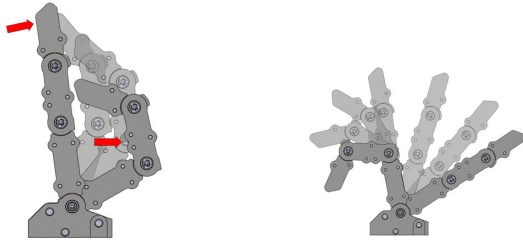


Fig. 6: Structure of an actuation assembly. It is composed by a BLDC motor and a low reduction-ratio transmission that contains two stages of pulley sets.

condition on the finger. If the finger is mainly loaded on the tip, the finger will be straight, which is good for grasping with finger tips, while if the load is mainly on the middle of the finger, the finger will be bent, and it will automatically shape itself to the best fit on the surface of the objective.

The specific arrangement and design of the extensor tendons make the finger follow a desired trajectory under zero load condition. When grasping, it is preferred to keep the finger straight until the finger touches the objective or the proximal phalanx reaches its limit of rotation during a grasping motion, as shown in Fig.7b, ensuring the largest workspace for each finger. Also, as discussed before, the finger shapes itself according to the loading condition, thus keeping the finger straight while approaching the objective helps the finger to shape itself to the best grasping shape upon contact when the grasper is going to grasp and hold the objective in hand, or reach its tip out for picking the objective with the fingertips when the objective is relatively small.



(a) Finger trajectory under different loading conditions.

(b) Finger trajectory under free loading conditions.

Fig. 7: The specific arrangement and design of the extensor tendons make the finger follow a desired trajectory under zero load condition.

This mechanical intelligence feature can be explained from the view of the flow of potential energy in and out the two extensor tendons.

The energy equality equation when flexing is as (1), where J is the kinematic energy in the system, E_p is the elastic potential energy, E_μ is the friction energy lost, W is the energy output to the environment, and M on the right side is the total energy from the actuator. E_g is the potential energy from gravity but it is so small that it can always be ignored.

E_p can be split into the potential energy stored in the springs, E_s and the potential energy stored in the elastic member between the distal and middle phalanx, E_k . E_s is associated with MCP joint and E_k is associated with PIP & DIP joints. E_μ is mainly introduced by the tendon contacting and sliding against the finger inner structure and it is relatively small comparing to M so it can be ignored.

$$J + E_p + E_g + W = M - E_\mu \quad (1)$$

Without loss of generality, we assume the finger moves quasi-statically under freeloading condition, and (1) becomes (2).

$$E_k + E_s = M \quad (2)$$

The distal phalanx extensor tendon elastic member and the tensile spring for the main extensor tendon are designed such that, without external forces and only by pulling the flexor tendon, it is significantly easier for the energy to flow into the tensile spring than the distal phalanx extensor tendon elastic member. This results in the proximal phalanx always bending prior to the middle and distal phalanxes, and only when the proximal phalanx is stopped by external force or the MCP joint reaches its limit will the middle and distal phalanxes then begin to bend.

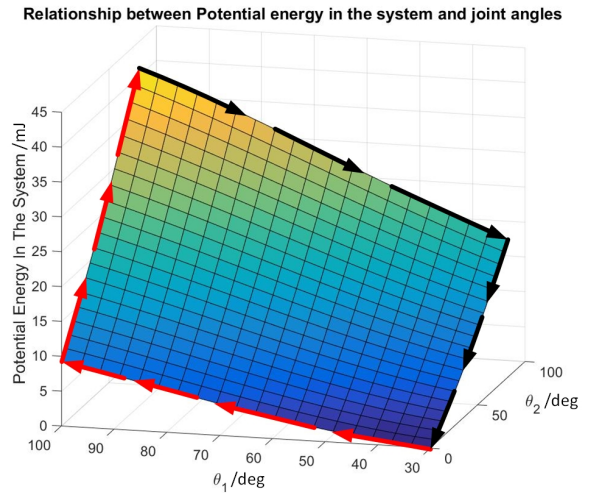


Fig. 8: Potential energy in the finger system regarding to the finger joint positions.

Shown in Fig. 8 is a plot of total potential energy in a finger as a function of θ_1 and θ_2 , which are the MCP joint angle and the PIP joint angle. This finger is a typical spring-mass-damping system, and for this kind of a mechanical system, the stable equilibria in most cases are coincident with local minimum potential energy points. In our finger system, as the flexor tendon is being pulled, energy is pumped into the system and distributed among the values on the left side of (1). Furthermore, the friction can be ignored when the flexor is being pulled by the actuator.

Besides external influences from the environment, the trajectory of the finger is determined by its potential energy

status, since the finger will always try to follow the trajectory that locally minimizes its energy state. In other words, when the flexor tendon is being pulled, the finger retracts along the trajectory in which the potential energy in the finger increases the slowest. Note that when the finger moves with a very high speed, the inertia of the finger itself then cant be ignored, and the inertial force from the finger acts like a external force. When the finger is moving with a relatively low speed and there is no external force from the environment on the finger, the retraction trajectory of the finger is exactly the trajectory marked with red arrows as shown in Fig. 8, which is the slowest trajectory for the potential energy in the system to increase.

When the finger releases, it should also try to follow the trajectory that minimizes its energy state. Thus, ideally, with friction in the system ignored, the finger should follow the reversed trajectory of the red-arrow marked retraction trajectory. However, in reality, instead of releasing the finger in the reversed sequence of retracting, the finger is released with MCP joint first, and then PIP and DIP joints. Due to the complex nonlinear damping that is involved in the releasing process, it is very difficult to come up with an accurate theoretical model for this, but the phenomenon will be analyzed comprehensively with the support of experiment results.

As mentioned in the mechanical design section, DANTE is designed for grasping tasks, thus the fingers are only actuated in flexing direction, and the recovery process is done by the elastic components in the system. The elastic components store potential energy for recovery process and consume the force provided by the actuator during flexion. For better gripping performance and power efficiency, the elastic components in our finger system are designed with relatively low spring constants. Thus, even though the friction in the system is small and ignorable when compared to the force from the actuator in flexion, it is not ignorable when the finger is recovering. In this case, the friction in the system increases the difficulty for the potential energy to release. The friction is mostly from the slipping contact between the tendons and the finger along the tendon routes. E_{μ} can be split into $E_{\mu s}$ which is associated with MCP joint movements and $E_{\mu k}$ which is associated with PIP&DIP joints movements, and the energy equality becomes:

$$E_k + E_s = E_{\mu k} + E_{\mu s} \quad (3)$$

From Fig. 5 we can tell that when only the MCP joint associated with θ_1 is rotating, there is almost no part of the tendons sliding against the finger inner structure, while releasing PIP and DIP joints associated with θ_2 and θ_3 will cause all the tendons to slide against the finger, generating significant friction forces. Thus, it seems to be much easier and faster for the finger system to go to a lower potential energy state by releasing MCP joint prior to the coupled PIP and DIP joints.

Experiments were conducted to support the theoretical analysis on mechanical intelligent in the finger system, and

the details and results of the experiments will be shown and discussed in later sections.

IV. CONTROL METHOD

Two different controllers have been developed for DANTE for different objectives. Velocity control is adopted for grasping tasks that requires high robustness and good tracking accuracy, while a compliance controller is developed for grasping tasks that require dedicated control of grasping force applied to the object. System controllers running at about 100Hz are developed in LabVIEW environment, as well as for serial communication to microcontrollers running FOC control on brushless motors, at a rate of 4kHz.

A. Velocity Control

We are currently only tracking the angular position of the tendon pulley, while the position and speed information from the encoder on the MCP joint has not been implemented into our controllers. The error of the pulley position is fed into a PD controller which generates a motor speed command input for the motor controller. The motor speed is then fed through a PID controller for the BLDC motor, and current control commands are then sent to the FOC controller for the BLDC motor. The control block diagram is as shown in Fig.9.

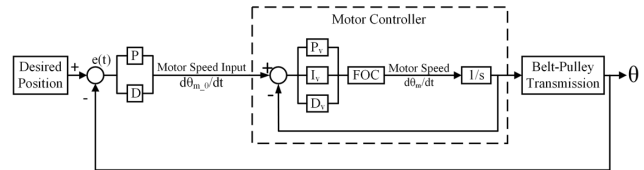


Fig. 9: Velocity control block diagram.

The finger controlled in this method appears to be very robust and precise in position tracking.

B. Compliance Control

In most of the grasping tasks that DANTE is designed for, controlling the pulley position and the MCP joint position is not necessary, since the mechanical intelligence in the finger system will automatically shape the finger into the best posture for holding the goal objects. Even though the pulley position is the same, the positions of all the three joints on the finger can be different for different objects. However, the MCP joint position and velocity is still being tracked, meaning the position and velocity of the PIP and the DIP joints can be calculated through kinematics. Forces applied through the finger were not quantified, but determined empirically, and since we rely on the torque current in the motor winding to reflect the force applied, it is very important for us to know the velocity and position of all the three joints in our compliance control, such that the back driving force from the springs and the elastic components and forces generated from the moment of inertia of the three phalanges can be known and compensated for. The following equation of motion [13] applies to the finger system:

$$B(q)\ddot{q} + C(q, \dot{q})\dot{q} + F\dot{q} + g(q) = u - J^T(q)h_e \quad (4)$$

Where q is the column vector of joint angular positions.

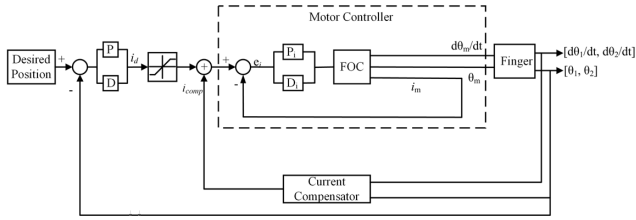


Fig. 10: Compliance control block diagram.

The mechanical intelligence property within the fingers made it possible to perform grasping tasks where the object location is not necessarily known in the grasper workspace.

The compliance control block diagram is as shown in Fig.10. The error on the tendon pulley position between the reference and current position is fed into a PD controller to generate a current control reference i_d . This current control reference i_d is then fed into a saturation filter to get the actual current control signal \hat{i}_d . The saturation filter is set to limit the torque current in the motor according to required force output.

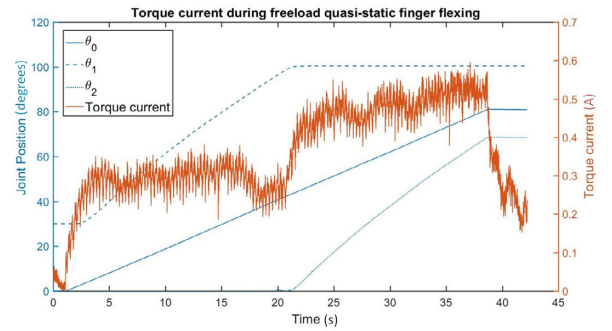
The speed and position information of the MCP joint and the pulley is used to calculate the forward kinematics of the finger system, and the position and speed of the joints are fed into a current compensator to calculate compensation for phalanges moment of inertia and elastic back driving force from the elastic member and the springs. Compensated current control signal is finally fed into the motor controller.

V. EXPERIMENTS, RESULTS AND DISCUSSION

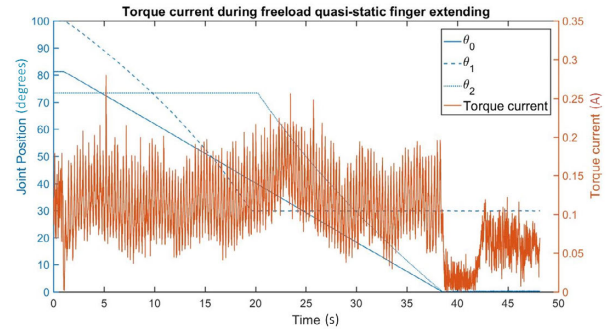
A. Free Load Finger Retraction & Extension

The free load finger retraction and extension experiments are done to collect experimental data to support the previous analysis on the mechanical intelligence property on the finger system. Both of finger retraction and extension experiments are done with a very low speed such that the moment of inertia can be ignored, and the torque current in the motor is recorded during the experiments.

Fig.11a shows the experiment results for flexing and extending. The torque current in the motor refers to the Y-axis on the right while all the angular position displacement of the joints and pulley refer to the Y-axis on the left. The pulley position and MCP joint position displacements are as read from the encoder on the joint while the PIP joint position is calculated from forward kinematics. There is no need to show the DIP joint position since it is coupled with PIP joint and those two joints always move together. By looking at the figure from finger flexing test, we can easily tell that during the whole flexing process, the MCP joint moved prior to the PIP & DIP joints, as the MCP joint started bending as soon as the pulley started pulling the tendon, while the PIP joint remained still until the MCP joint has reached its mechanical limit and stopped bending. The data also show that less current is required to drive the MCP joint than the PIP & DIP joints. On the other hand, the finger extending experiment result shows that during the whole



(a) Flexing



(b) Extending

Fig. 11: Torque reading from the actuator in amps during freeload quasi-static finger retraction and extension.

process the motor torque current varies very little regardless of where the joints are, and the torque current is almost the basic current requirement to drive the motor to rotate at this speed, as shown in Fig.11b.

Still, it is worth noting that the torque current in the motor is slightly smaller when the MCP joint is fully released and the PIP & DIP joints are extending. This means that when the finger is extending, the back driving force from releasing the potential energy in the springs and elastic member is just able to overcome the friction in the system, and potential energy in the finger system is released slightly faster when releasing the MCP joint than when releasing the PIP & DIP joints. All this experiment data support and confirm our previous analysis on the energy flow theory behind the mechanical intelligence that the finger system presents.

B. Grasping Test

The mechanical intelligence that is designed and embedded in the finger systems on DANTE enables the finger to follow a desired trajectory under free-load condition while automatically configuring into the best posture for the goal object when performing grabbing task. As the trajectory control function of the mechanical intelligence was discussed in the previous sections, the automatic object fitting ability and the general grasping ability of the system is tested and evaluated below.

As introduced in the design section earlier in this paper, DANTE has two fingers that can rotate mirrored. This function provides DANTE with three general finger postures:

parallel posture with all fingers parallel with each other, mirrored posture with the two movable fingers mirrored with each other and perpendicular with the stationary finger, and axisymmetric posture with all the three fingers axisymmetric with each other. These three modes can cover almost all grasping cases, and though the movable fingers can move to any arbitrary position between the parallel posture and the mirrored posture, configurations other than the mentioned three are very rarely used.

Numerous grabbing tests are done, and several representative scientific grasping scenarios [14] used to fully evaluate the grasping capability of DAnTE are shown in Fig.12. The fingers can automatically fit to the outline of the goal object very well, and for the same object, unique and optimized grasping configurations of the finger joints are applied automatically for different grasping methods. For instance, very different finger joints configurations are applied when grabbing a red ball firmly in hand or holding the same ball with finger tips. The configuration is also different when it comes to holding a smaller ball with a precision grasp or a screw driver with finger tips or heavy wrap. For these tasks, the axisymmetric posture is applied. When grabbing objects with a long profile, such as a screwdriver, a bottle or the handle of a power tool, the parallel posture comes handy. When it comes to objects with a flat and thin profile, such as a card, or small objects that is hard to be picked up with three fingers, two finger pinch will be applies. Note that figure. 12 has been modified from the original figure in [14], since three-finger hand can act very differently to a human-like five-finger hand for some specific tasks. For instance, while there are not as many different ways of handling prismatic objects, there are also some configurations unique to the three-finger hand, such as using the thumb finger as axial support when holding a mug full of water or using the palm to provide axial support to firmly hold a small screwdriver. These two ways of handling prismatic objects precisely can also provide some in-hand manipulation that may be needed when using the object tool.

C. Dexterous Grasping

The goal of this experiment is to test DAnTEs ability of dexterous force controlled grasping and evaluate the effectiveness of the inherent compliance on the fingers introduced by using quasi direct-drive actuators. Dexterous force controlled grasping over delicate objects is very challenging for all robotic hands. The compliance controller we have developed is used in this experiment and the challenging task we have chosen for DAnTE is to approach and grasp a fresh potato chip as shown in Fig.13 with a high speed, while not breaking the potato chip.

In this experiment, the three fingers are asymmetric and play very similar roles, thus we only need to look at the experiment data from one finger to sufficiently know about the other two fingers and the whole robotic hand. Shown in Fig.14 is the recorded experiment data of one finger. The grasping task was finished within a quarter of a second. The peak of the torque current at the beginning is the sudden

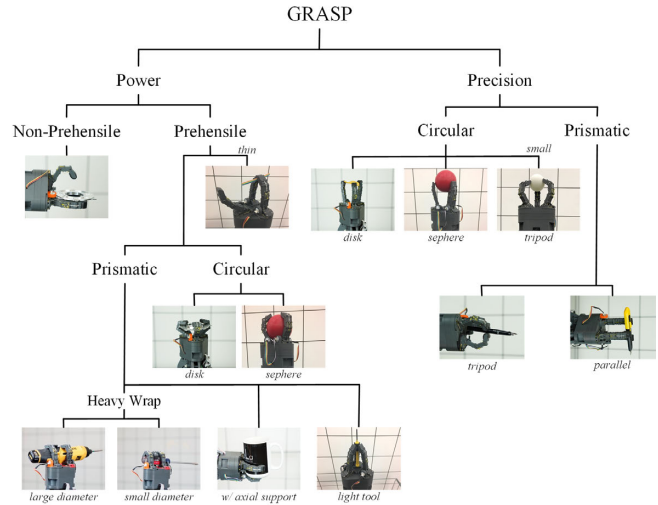


Fig. 12: Evaluation of the grasping capability of DAnTE. The fingers can automatically fit to the outline of the goal object very well, and for the same object, unique and optimized grasping configurations of the finger joints are applied automatically for different grasping methods.



Fig. 13: DAnTE grasping a potato chip.

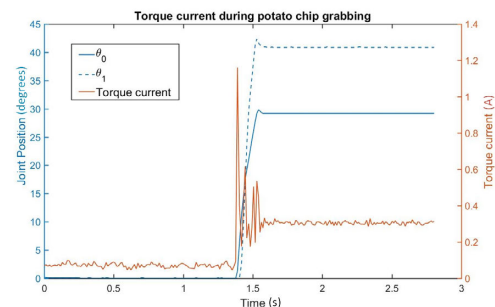


Fig. 14: The corresponding torque current in one of the actuators during the potato chip grabbing manipulation.

acceleration of the finger to a desired high speed, and the finger stopped moving once it made contact with the potato chip and kept a preset light grasping force. However, there is still a little overshoot in the system. It might be caused by that even though the motor controller runs at 4kHz, the system control loop can only run at about 100Hz. We hope to eliminate the overshoot by increasing the frequency of the system control loop in the future.

VI. CONCLUSIONS

In this paper, we present a three finger under actuated robotic hand designed with embedded mechanical intelligence and current based live force sensing and inherent compliance. Each finger on DANTE is under actuated and driven by only one actuation module. The actuation modules are high torque BLDC motors with a small speed reduction ratio of about only 1:8 and provides excellent inherent compliance to all the fingers, making it possible to directly sense and control the force on the finger by monitoring and controlling the torque current in the motor. The tendon driven fingers on DANTE are a simplified biomimetic design of human fingers. While being under actuated, the trajectory of the finger is controlled by the mechanical intelligence such that when approaching the goal object, the finger always follows a preferred trajectory that goes through most of its reachable area. The mechanical intelligence also provides the finger with automatic object fitting ability, which makes the finger to always use the best gesture for grabbing the object.

We also tried to look at the mechanical intelligence feature from the angle of energy and provided a potential energy flow theory to explain mechanical intelligence feature. The theory is proved with experiment on DANTE system.

A velocity controller is designed and applied to achieve precise position tracking and a compliance controller is designed and applied on DANTE system for grabbing tasks with high requirement on force control ability. DANTE has also shown great performance on dexterous grasping, as we have discussed the experiment on grabbing a fragile potato chip with three fingers at a high speed without breaking the object.

VII. FUTURE WORK

In the future, we will perform many updates and changes to improve the system. On the hardware side, the fingers will be made of different materials and methods such as CNC aluminum, SLA 3D print resin and other engineering plastics to optimize and improve the strength, weight and performance of the hand. The actuation modular will be further developed, redesigned and repackaged to make it more compact and efficient. Other design of the finger such as fingers using linkages will also be tested and fully actuated fingers instead of under actuated ones can also be made to compare. On the software side, we will be improving the system control loop frequency to further improve the compliance control on DANTE. In hand manipulation will also be implemented onto this robotic hand system. Furthermore, we are also looking at using the finger joint position information and grabbing force

information to roughly guess or recognize the object being grabbed in DANTE. It is also planned to integrate this robotic hand with a robot arm and carry out further researches.

REFERENCES

- [1] M. Grebenstein, A. Albu-Schäffer, T. Bahls, M. Chalon, O. Eiberger, W. Friedl, R. Gruber, S. Haddadin, U. Hagn, R. Haslinger, *et al.*, "The dlr hand arm system," in *Robotics and Automation (ICRA), 2011 IEEE International Conference on*. IEEE, 2011, pp. 3175–3182.
- [2] V. Kumar, Z. Xu, and E. Todorov, "Fast, strong and compliant pneumatic actuation for dexterous tendon-driven hands," in *Robotics and Automation (ICRA), 2013 IEEE International Conference on*. IEEE, 2013, pp. 1512–1519.
- [3] A. M. Dollar and R. D. Howe, "Simple, robust autonomous grasping in unstructured environments," in *Robotics and Automation, 2007 IEEE International Conference on*. IEEE, 2007, pp. 4693–4700.
- [4] T. Laliberté, L. Birglen, and C. Gosselin, "Underactuation in robotic grasping hands," *Machine Intelligence & Robotic Control*, vol. 4, no. 3, pp. 1–11, 2002.
- [5] N. T. Ulrich, "Grasping with mechanical intelligence," *Technical Reports (CIS)*, p. 846, 1989.
- [6] J. Phillips, *Freedom in Machinery: Introducing Screw Theory*; Jack Phillips. Cambridge University Press, 1984.
- [7] J. Tegin and J. Wikander, "Tactile sensing in intelligent robotic manipulation—a review," *Industrial Robot: An International Journal*, vol. 32, no. 1, pp. 64–70, 2005.
- [8] H. Yousef, M. Boukallel, and K. Althoefer, "Tactile sensing for dexterous in-hand manipulation in robotics—a review," *Sensors and Actuators A: physical*, vol. 167, no. 2, pp. 171–187, 2011.
- [9] D.-H. Lee, U. Kim, H. Jung, and H. R. Choi, "A capacitive-type novel six-axis force/torque sensor for robotic applications," *IEEE Sensors Journal*, vol. 16, no. 8, pp. 2290–2299, 2016.
- [10] M. H. Raibert and J. J. Craig, "Hybrid position/force control of manipulators," *Journal of Dynamic Systems, Measurement, and Control*, vol. 103, no. 2, pp. 126–133, 1981.
- [11] S. Seok, A. Wang, D. Otten, and S. Kim, "Actuator design for high force proprioceptive control in fast legged locomotion," in *Intelligent Robots and Systems (IROS), 2012 IEEE/RSJ International Conference on*. IEEE, 2012, pp. 1970–1975.
- [12] V. Bundhoo and E. J. Park, "Design of an artificial muscle actuated finger towards biomimetic prosthetic hands," in *Advanced Robotics, 2005. ICAR'05. Proceedings., 12th International Conference on*. IEEE, 2005, pp. 368–375.
- [13] B. Siciliano, L. Sciacivico, L. Villani, and G. Oriolo, *Robotics—Modelling, Planning and Control. Advanced Textbooks in Control and Signal Processing Series*. London, UK: Springer-Verlag, 2009.
- [14] M. R. Cutkosky, "On grasp choice, grasp models, and the design of hands for manufacturing tasks," *IEEE Transactions on robotics and automation*, vol. 5, no. 3, pp. 269–279, 1989.